Global organization of spiral structures in biparameter space of dissipative systems with Shilnikov saddle-foci

Roberto Barrio, Fernando Blesa, Sergio Serrano, and Andrey Shilnikov

Phys. Rev. E **84**, 035201 — Published 19 September 2011

DOI: 10.1103/PhysRevE.84.035201

Global organization of spiral structures in bi-parameter space of dissipative systems with Shilnikov saddle-foci

Roberto Barrio,[1,*] Fernando Blesa,[2] Sergio Serrano,[1] and Andrey Shilnikov[3]

[1] *Departamento de Matemática Aplicada and IUMA. University of Zaragoza. E-50009. Spain.*
[2] *Departamento de Física Aplicada. University of Zaragoza. E-50009. Spain.*
[3] *Neuroscience Institute and Department of Mathematics and Statistics, Georgia State University, Atlanta 30303, USA*

We reveal and give a theoretical explanation for spiral-like structures of periodicity hubs in the bi-parameter space of a generic dissipative system. We show that organizing centers for "shrimp"-shaped connection regions in the spiral structure are due to the existence of L. Shilnikov homoclinics near a codimension-2 bifurcation of saddle-foci.

PACS numbers: 05.45.Ac, 05.45.Pq

Over recent years, a great deal of experimental studies and modeling simulations have been directed toward the identification of various dynamical and structural invariants to serve as key signatures uniting often diverse nonlinear systems into a single class.

One such class of low order dissipative systems has been identified to possess one common, easily recognizable pattern involving spiral structures, called the periodicity hub, along with shrimp-shaped domains in a biparametric phase space [1, 2]. Such patterns turn out to be ubiquitously alike in both time-discrete [3, 4] and time-continuous systems [5–7], as well as in experiments [1, 8].

Despite the overwhelming number of studies reporting the occurrence of spiral structures, there is still little known about the fine construction details and underlying bifurcation scenarios for these patterns. In this Brief Communication we study the genesis of the spiral structures in two exemplary, low order systems and reveal the generality of underlying global bifurcations. We will demonstrate that such parametric patterns along with shrimp-shaped zones are the key feature of systems with homoclinic connections involving saddle-foci meeting the single Shilnikov condition [9]. The occurrence of this bifurcation causing complex dynamics is common for a plethora of dissipative systems, describing (electro)chemical reactions [10], population dynamics [11], electronic circuits and nonlinear optics [2, 8, 12].

The first paradigmatic example is the canonical Rössler system [13]:

$$\dot{x} = -(y+z), \quad \dot{y} = x + ay, \quad \dot{z} = b + z(x-c), \qquad (1)$$

with two bifurcation parameters a and c (we fix $b = 0.2$). For $c^2 > 4ab$ the model has two equilibrium states, $P_{1,2}(ap_\pm, -p_\pm, p_\pm)$, where $p_\pm = (c \pm \sqrt{c^2 - 4ab})/2a$. This classical model exhibits the spiral and screw chaotic attractors after a period doubling cascade followed by the Shilnikov bifurcations of the saddle-focus P_2.

The second example is the Rosenzweig-MacArthur model [11, 14]:

$$\begin{aligned} \dot{x} &= x\,[\,r\,(1 - x/K) - 5y/(1+3z)\,]\,, \\ \dot{y} &= y\,[\,5y/(1+3x) - z/10(1+2y) - 0.4\,]\,, \\ \dot{z} &= z\,[\,y/10(1+2y) - 0.01\,]\,, \end{aligned} \qquad (2)$$

for a tritrophic food chain composed of a logistic prey, x, a Holling type II predator, y, and a top-predator, z; two bifurcation parameters K and r control the regrowth rates of the prey [11].

Bi-parametric screening the Rössler (panels A-B) and food chain (panels C-D) models unveils a stunning universality of the periodicity hubs in the bifurcation diagrams shown in Fig. 1 of both models. Each diagram is built on a dense grid of 1000×1000 points in the parameter plane. Solutions of the models were integrated using the high precision ODE solver TIDES [15]. The color bars on the right in Fig. 1 yield a spectrum of the Lyapunov exponents. Panels (A) and (C) of the figure reveal the characteristic spiral patterns, where dark and light colors discriminate between the regions of regular and chaotic dynamics corresponding to a zero and positive maximal Lyapunov exponent λ_1, respectively. Panels (B) and (D) show the enhanced fine structures of the bifurcation diagrams of the models, due to variations of both Lyapunov exponents λ_1 and λ_2. The white stripes expose shrimps-shaped areas (within red-boxes) on the dark background of the regular ($\lambda_1 = 0$) region, as well as in the multicolored region corresponding to complex dynamics ($\lambda_1 > 0$).

The panels are overlaid with (thin blue) curves (obtained using [16]) that correspond to saddle-node (or fold) bifurcations of periodic orbits. These curves demarcate the stability windows from chaotic regions within the spiral structure which are either via the intermittency of type I boundary crisis [6], or due to a period doubling bifurcation. In the case of the Rössler model, the saddle-node curves spiral onto a F(ocal) point [1, 2] at $(a, c) = (0.1798, 10.3084)$. This F-point seems to be the turning point of a bifurcation curve (thick black) corresponding to a formation of a homoclinic loop of the saddle-focus, P_2, of the Rössler model. Another curve

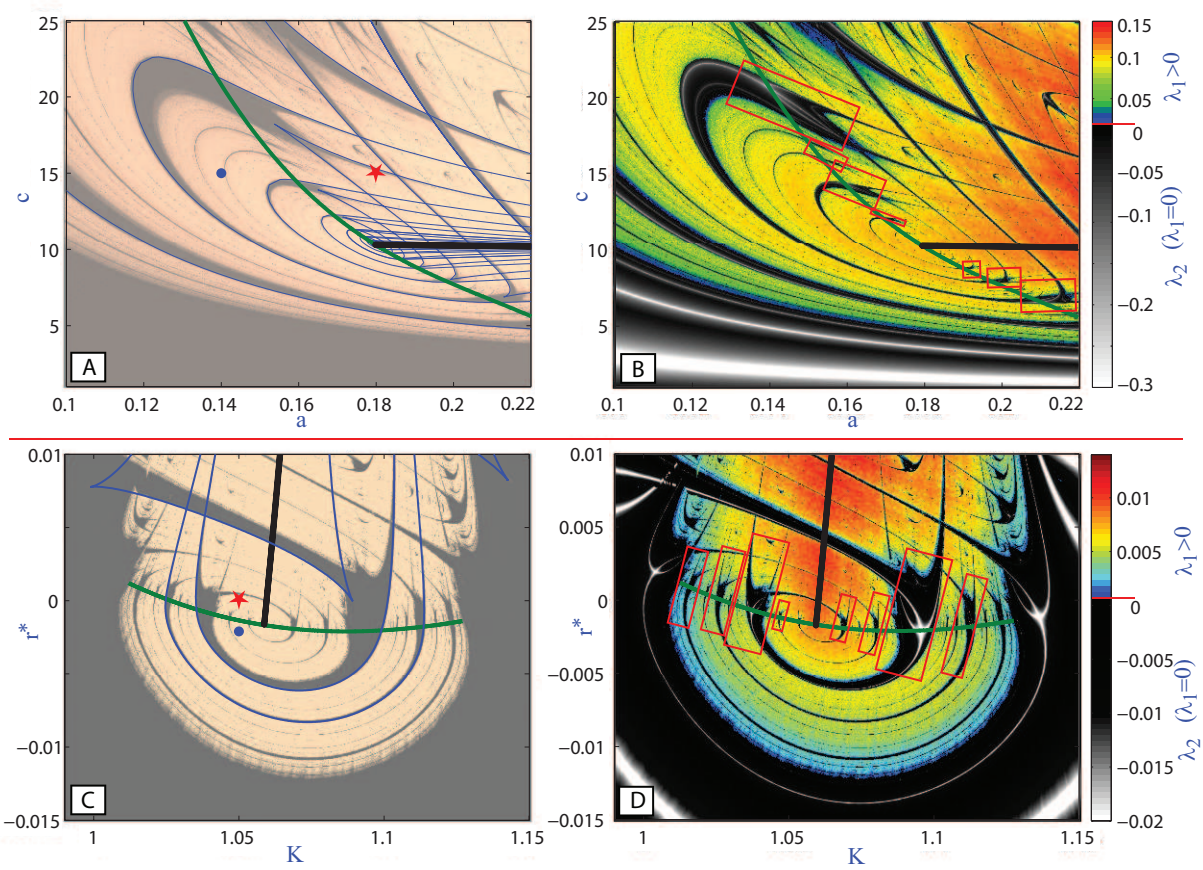

Figure 1. (Color online) Spirals and "shrimps" in the 1000×1000 grid biparametric bifurcation diagrams for the Rössler (A-B) and tritrophic food chain (C-D) models. The F-point of the hub is located at $(a, c) = (0.1798, 10.3084)$ and $(K, r^*) = (1.0587, -1.6285 \cdot 10^{-3})$ (resp.). The color bars for the Lyapunov exponent range identify the regions of chaotic and regular dynamics. For visibility the parameter plane of the food chain model is untwisted by transformation $r^* = r + 0.11(K - 1)/0.14 - 0.83$. Left monochrome panels are superimposed with bifurcation curves: thin blue for saddle-nodes, and thick black for homoclinic bifurcations of saddle-foci. The medium-thick green boundary determines a change in the topological structure of chaotic attractors from spiral (at •) to screw-shaped (at ⋆).

(medium-thick green) passes (up to our numerical precision) through the F-point: crossing it rightward the chaotic attractor changes the topological structure from spiral to screw-shaped. This curve has been singled out of a 1000×1000 grid of points in the parameter plane. In what follows we will describe the topological algorithms applied for detecting this boundary, which are based on the examination of the number of critical points and monotonicity intervals in corresponding 1D Poincaré return maps [6, 17]. This transition is completely different from one considered in [17], where maps with an increasing number of branches are detected in other parametric ranges [6].

The topological structure of the Rössler attractor can be described in terms of topological templates [18]. A template is a branched two-dimensional manifold to which any periodic orbits (space curves in $\mathbb{R}^3$) in the attractor are projected without changing their (self) knotting and (mutually) linking invariants. Practically, the template may be derived using a Poincaré return map defined on successive local maxima, $y(i)$, of the y-coordinate of trajectories on the chaotic attractor for further examining the knots of the unstable periodic orbits (UPOs) foliating the attractor. The map allows for the determination of the number of branches of the template, which is associated with the number of monotone components in the map graph. The study of the *signed crossings* of the UPOs uniquely determine topological template of the chaotic attractor [18]. So, the *spiral attractor* in the Rössler model at $a = 0.14$ (the point labeled by "•" in the diagram in Fig. 1(A)) generates a 1D unimodal map shown in Fig. 2 (top). The single critical point of the map graph determines the boundary between the normal and twisted (resp.) stripes. This lets a symbolic description be naturally introduced for the map using two symbols, 0 and 1, for corresponding branches. In the case of the

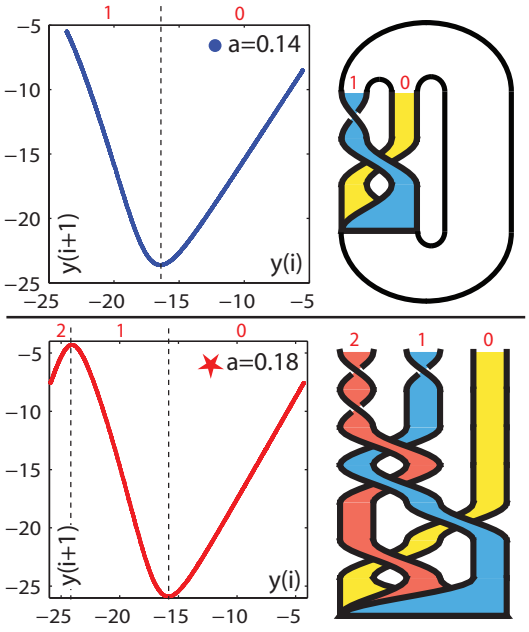

Figure 2. (Color online) Poincaré return maps in the left panels for the spiral and screw-shaped (resp.) chaotic attractors in the Rössler model (1) at $a = 0.14$ and 0.18 for $c = 15$. Right panels show the corresponding topological templates.

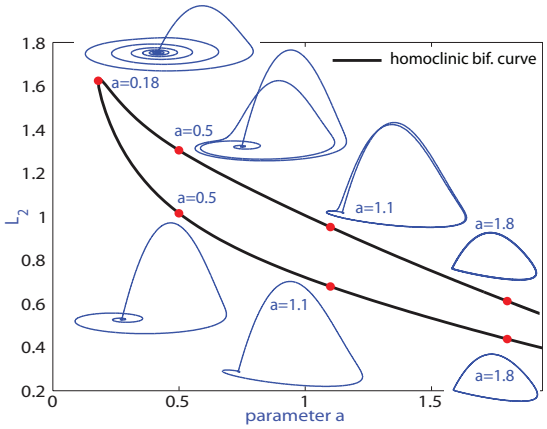

Figure 3. (Color online) Transformation of homoclinic orbits to the saddle-focus, P_2, in the Rössler system: AUTO L_2-norm of the orbit is plotted against the bifurcation parameter a. The turning point terminates two branches: bottom corresponding to the primary homoclinic loop, while the top one corresponds to the secondary loop with an additional round. Homoclinic orbits are sampled at the indicated points.

screw attractor at $a = 0.18$ (the point labeled by "$\star$" in the diagram in Fig. 1(A)), the corresponding map in Fig. 2 (bottom) has a bimodal graph with two critical points. Here the symbolic dynamics can be defined using three symbols: {0, 1, 2}. The addition of the second critical point in the map is a direct indication that the spiral attractor changes topology. This criteria was used to locate the corresponding boundary (medium-thick green line) that separates the existence regions of the attractors of both types in the bifurcation diagram in Fig. 1. Notice that this boundary passes right through the F-point.

The linking matrices, which contain necessary topological information for the spiral and screw attractors of the Rössler model are given by:

$$M_{\rm sp} = \begin{pmatrix} 0 & -1 \\ -1 & -1 \end{pmatrix}, \qquad M_{\rm sc} = \begin{pmatrix} 0 & -1 & -1 \\ -1 & -1 & -2 \\ -1 & -2 & -2 \end{pmatrix}, \qquad (3)$$

using the same notation as [17]. The diagonal elements in each matrix are the sum of the signed half-twists in each branch. The off-diagonal elements are the sum of the oriented crossings between the branches. Thus, in the spiral attractor we have a 0 entry implying that the right branch (0) has no twists (Fig 2(A)), and the middle branch (1) (left branch (2)) has a half-twist (the entry -1 (or -2)). The other -1 entries indicate that two branches of the topological template cross once only.

The (thick black) bifurcation curve in Fig. 1(A) corresponds to a formation of the primary homoclinic orbit to the saddle-focus, P_2, of topological type (1,2), i.e. with 1D stable and 2D unstable manifolds, in the Rössler model (1). Depending on the magnitudes of the characteristic exponents of the saddle-focus, the homoclinic bifurcation can give rise to the onset of either rich complex or trivial dynamics in the system [9, 19]. The cases under considerations meet the Shilnikov conditions and hence the existence of a single homoclinic orbit implies chaotic dynamics in the models within the parameter range in the presented diagrams. The magnification of the corresponding bifurcation curve in the diagram (Fig. 1(A,B)) reveals that what appears to be as a single bifurcation curve has two branches (Fig. 3). This curve has a U-shape which turning point seems to be at the F-point. To examine the U-shape in detail we plot the bifurcation curve in terms the L_2-norm [16] of the homoclinic orbit against the bifurcation values of the parameter a (for periodic solutions $U(t)$, the L_2-norm is defined as $\|U\|_2 = \sqrt{\int_0^1 \|U(t)\|^2 dt}$, where the independent variable t is scaled to $[0, 1]$). Fig. 3 shows that the F-point terminates two branches of homoclinic loops or, alternatively, serve as a turning for the homoclinic branches.

Fig. 4 outlines a structure of the bifurcation unfolding around the spiral hub [7]. Inset (A) depicts a number of the identified saddle-node bifurcation curves originating from codimension-2 points, labeled as B(elyakov), toward the spiral hub in the (a, c)-parameter plane for the Rössler model. At these B-points, the saddle with real characteristic exponents becomes a saddle-focus for smaller values of the parameter a. The unfolding of this bifurcation is known [20] to contain bundles of countable many curves corresponding to saddle-node and period

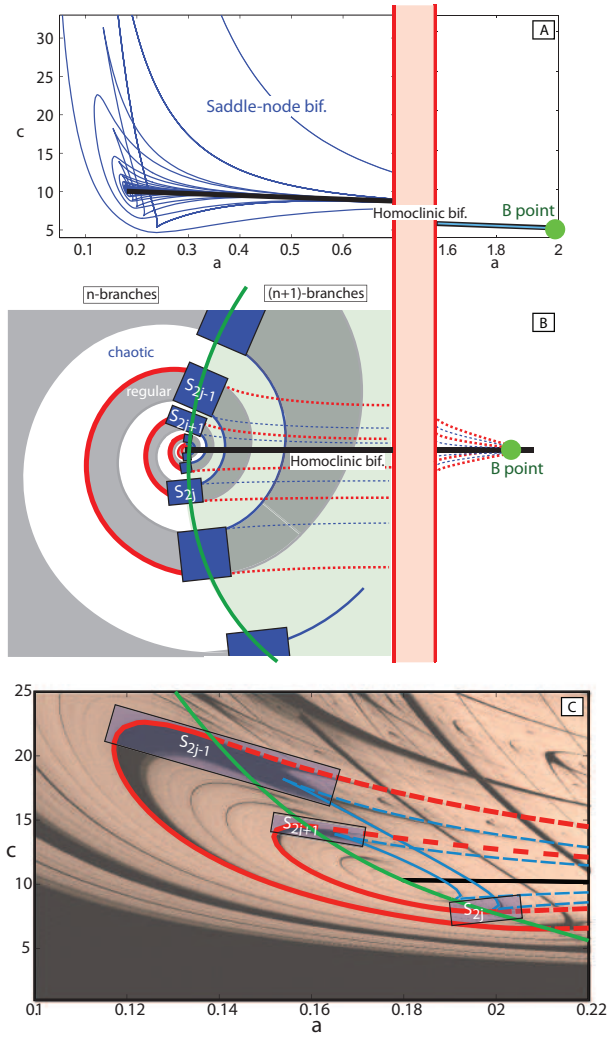

Figure 4. (Color online) Outline of the spiral structures: (A) two kinds, folded and cusp-shaped of saddle-node bifurcation curves for the Rössler model originating from the cod-2 homoclinic B-point. (B) phenomenological sketch of the spiral hub formed by the "shrimps." (C) Magnification of the bifurcation portrait of the spiral hub, overlaid with principal folded (thick red) and cusp-shaped (thin blue) bifurcation curves setting the boundaries for largest "shrimps" in the Rössler model.

doubling bifurcations of periodic orbits [14], as well as to various secondary homoclinic bifurcations of the saddle-focus. Indeed, both B- and F-points together globally determine the structure of the (a, c)-bifurcation portrait of the Rössler model. Fig. 4(B) sketches phenomenologically a caricature of the bifurcation structure of the spiral hub along with "shrimps." In it, the saddle-node bifurcation curves originating from the B-point demarcate the boundaries of "shrimps" near the spiral hub, Indeed, the hub can generate an infinite chain of "shrimps" [2, 10]. A zoom of the Rössler bifurcation diagram the in panel C in Fig.4 depicts a few such shrimps, S_{2j} and $S_{2j\pm1}$, that are singled out by the saddle-node curves (solid red) folding back around the F-point in the existence region of the spiral attractor (to the left from the corresponding boundary (green) passing through the F-point). The cusp-shaped saddle-node bifurcation curves (light blue) join the successive S_{2j-1}-th and S_{2j}-th shrimps in the existence region of the screw-type attractor (here, the subscript j stands for an ordinal number of nearby shrimps). Thus, both fold- and cusp-shaped bifurcation curves of saddle-node periodic determine the local structure of the hub and the "shrimps." The latter serve as connection centers between hubs that contribute towards the formation of characteristic spiral structures in the bifurcation diagram of the system.

We have presented a generic scenario for the formation of the spiral structures and "shrimps" in the biparameter space of a system with a Shilnikov saddle-focus. The skeleton of the structure is due to fold- and cusp-shaped bifurcation curves of saddle-node periodic orbits that accompany the homoclinics of the saddle-focus. These bifurcation curves distinctively shape the "shrimp" zones in the vicinity of the spiral hub. In the Rössler model, these bifurcation curves originate from the codimension-2 Belyakov point corresponding to the transition to the saddle-focus from a simple saddle. The common feature of the spiral hub in the Rössler and the tritrophic food chain models is the F-point at the center of the spiral structure that gives rise to the alternation of the topological structure of the chaotic attractor transitioning between the spiral and screw-like types. The findings let us hypothesize about a universality of the structure of the spiral hubs in similar systems with chaotic attractors due to homoclinics of the Shilnikov saddle-focus.

The authors R.B., F.B. and S.S. acknowledge the support from the Spanish Research projects MTM2009-10767 and AYA2008-05572, and A.S. acknowledges NSF grant DMS-1009591 and RFFI Grants No. 08-01-00083.

* Corresponding author: rbarrio@unizar.es

[1] C. Bonatto, J. C. Garreau, and J. A. C. Gallas, Phys. Rev. Lett. **95**, 143905 (2005).
[2] C. Bonatto and J. A. C. Gallas, Phys. Rev. Lett. **101**, 054101 (2008).
[3] J. A. C. Gallas, Phys. Rev. Lett. **70**, 2714 (1993).
[4] Y. Zou, M. Thiel, M. C. Romano, J. Kurths, and Q. Bi, Internat. J. Bifur. Chaos Appl. Sci. Engrg. **16**, 3567 (2006); E. N. Lorenz, Phys. D **237**, 1689 (2008).
[5] J. A. C. Gallas, Internat. J. Bifur. Chaos Appl. Sci. Engrg. **20**, 197 (2010).
[6] R. Barrio, F. Blesa, and S. Serrano, Phys. D **238**, 1087 (2009).
[7] P. Gaspard, R. Kapral, and G. Nicolis, Journal of Statistical Physics **35**, 697 (1984).
[8] R. Stoop, P. Benner, and Y. Uwate, Phys. Rev. Lett. **105**, 074102 (2010); V. Castro, M. Monti, W. B. Pardo,

J. A. Walkenstein, and E. Rosa, Jr., Internat. J. Bifur. Chaos Appl. Sci. Engrg. **17**, 965 (2007).
[9] L. P. Shilnikov, Sov. Math. Dokl. **6**, 163 (1965); L. P. Shilnikov, A. L. Shilnikov, D. Turaev, and L. O. Chua, *Methods of qualitative theory in nonlinear dynamics. Part II* (World Scientific Publishing Co. Inc., 2001).
[10] M. A. Nascimento, J. A. C. Gallas, and H. Varela, Phys. Chem. Chem. Phys. **13**, 441 (2011).
[11] A. Hastings and T. Powell, Ecol. **72**, 896 (1991); Y. A. Kuznetsov, O. De Feo, and S. Rinaldi, SIAM J. Appl. Math. **62**, 462 (2001).
[12] J. G. Freire and J. A. C. Gallas, Phys. Rev. E **82**, 037202 (2010).
[13] O. E. Rössler, Phys. Lett. A **57**, 397 (1976).
[14] P. Hogeweg and B. Hesper, Comp. Biol. Med. **8**, 319 (1978); Y. A. Kuznetsov and S. Rinaldi, Math. Biosci. **134**, 1 (1996).
[15] A. Abad, R. Barrio, F. Blesa, and M. Rodríguez, TIDES software: http://gme.unizar.es/software/tides (2010).
[16] E. J. Doedel, R. C. Paffenroth, A. R. Champneys, T. F. Fairgrieve, Y. A. Kuznetsov, B. E. Oldeman, B. Sandstede, and X. J. Wang, AUTO2000: http://cmvl.cs.concordia.ca/auto (2011).
[17] C. Letellier, P. Dutertre, and B. Maheu, Chaos **5**, 271 (1995).
[18] R. Gilmore, Rev. Modern Phys. **70**, 1455 (1998); R. Gilmore and M. Lefranc, *The topology of chaos* (John Wiley & Sons, New York, 2002).
[19] P. Gaspard and G. Nicolis, J. Statist. Phys. **31**, 499 (1983).
[20] A. R. Champneys and Y. A. Kuznetsov, Internat. J. Bifur. Chaos Appl. Sci. Engrg. **4**, 785 (1994); L. A. Belyakov, Mat. Zametki **28**, 911 (1980).